THE JOURNAL OF PHYSICAL CHEMISTRY B

Article

pubs.acs.org/JPCB

Lipid Flip-Flop in Binary Membranes Composed of Phosphatidylserine and Phosphatidylcholine

Krystal L. Brown and John C. Conboy*

Department of Chemistry, University of Utah, 315 South 1400 East, Salt Lake City, Utah 84112, United States

ABSTRACT: The kinetics and thermodynamics of lipid flip-flop in bilayers composed of 1,2-dipalmitoyl-*sn*-glycero-3-phospho-L-serine (DPPS) and 1,2-distearoyl-*sn*-glycero-3-phosphocholine (DSPC) were studied using sum-frequency vibrational spectroscopy. The kinetics of DSPC and DPPS flip-flop were examined as a function of temperature and bilayer composition. The rate of DSPC flip-flop did not exhibit any significant dependence on bilayer composition while the rate of DPPS flip-flop was inversely dependent on the mole fraction of DPPS. The transition-state thermodynamics for DSPC and DPPS lipids in these mixed bilayers were determined in order to identify the energetic impact of the phosphatidylserine headgroup on lipid flip-flop. The thermodynamics for the DSPC component remained statistically identical to bilayers composed entirely of DSPC. The activation energy for the DPPS component showed a linear correlation with the mole fraction of DPPS for all bilayer compositions. The enthalpy and entropy for DPPS flip-flop did not increase linearly with the fraction of DPPS but did directly correlate with the molecular area. The DPPS component also exhibited enthalpy−entropy compensation which suggests that lipid hydration may play a significant role in membrane dynamics.

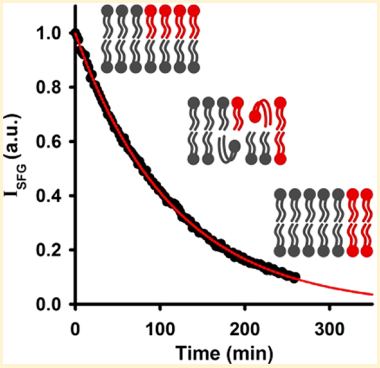

INTRODUCTION

The plasma membrane of eukaryotic cells contains a unique composition of proteins and lipids which form an optimal interface between the intracellular and extracellular matrices. In addition to the complex milieu of lipids and proteins, the membrane is marked by a heterogeneous distribution of phospholipids in each leaflet of the membrane. For example, the negatively charged phosphatidylserine (PS) headgroup lipids, which comprise only 3−15% of all cellular phospholipids,[1−3] are found exclusively in the cytosolic leaflet[2−4] where they modulate the localization and activity of many membrane-bound proteins, including protein kinase C.[5,6] Exposure of PS lipids to the extracellular leaflet triggers a variety of concentration-dependent responses ranging from blood coagulation[7−11] and vesicle formation[9,10,12] to phagocyte recognition and apoptosis.[1,13−15] Furthermore, unregulated changes in the PS lipid distribution are implicated in diseases such as diabetes,[16,17] sickle cell anemia,[18,19] and the congenital bleeding disorder Scott syndrome.[20,21]

Despite the numerous and severe implications of both regulated and unregulated PS lipid asymmetry, the mechanism by which the PS distribution is maintained is not well understood. This mechanism must be a complex interplay between native lipid dynamics, retentive forces that immobilize lipids,[9,11,22] and protein-regulated lipid transport.[4,23−25] Although a great deal of research has been aimed at understanding this mechanism, the external forces which modulate lipid location have been targeted almost exclusively. Native lipid translocation between membrane leaflets, or lipid flip-flop, is an integral component of cellular PS lipid distribution that has remained particularly obscured due to methodological limitations.

Traditionally, the localization of PS lipids has been studied indirectly using PS binding molecules or PS lipid analogues. The former method has successfully quantified PS lipid distribution and PS externalization in apoptotic and diseased cells.[2,18,26] The proteins Annexin A5 and Lactadherin are current favorites, possessing high PS specificity.[5,18,26] However, the kinetics of protein binding perturbs native lipid behavior, thereby precluding the use of this method to study native PS lipid translocation. PS lipid analogues containing a short acyl chain (6−12 carbons) terminated with a fluorescent or spin-labeled molecule[5,27−30] have been incorporated into cellular membranes to assess the impact of PS lipid transporter proteins on PS lipid distribution using standard fluorescence or spin techniques.[27,30] The use of such probes is not suitable to study flip-flop kinetics as both the short acyl chain and the chemical alteration of the PS lipid by the exogenous probe can have a drastic impact on the measured rates of lipid translocation.[31,32] We have previously shown that the measured dynamics of lipid analogues are not representative of native lipid behavior.[33]

Recently, label-free methods have been used to study lipid dynamics in vesicles by shape changes[24,34] and small-angle neutron scattering[35] as well as in planar supported lipid bilayers (PSLBs) using AFM.[36] One label-free method that is particularly well suited to study lipid flip-flop is sum-frequency vibrational spectroscopy (SFVS). SFVS is sensitive to molecular symmetry and can be used to directly monitor changes in lipid distribution in real time.[31−33] Previous studies using SFVS to examine the kinetics of lipid flip-flop have reported that bilayer

Received: September 27, 2013
Revised: November 7, 2013
Published: November 7, 2013

composition, packing, and phase each play a significant role in lipid dynamics.[31−33,37,38] These previous studies underscore the need to determine the influence of the PS headgroup on lipid translocation in membranes.

In the work presented here, the dynamics of 1,2-dipalmitoyl-*sn*-glycero-3-phospho-L-serine (DPPS) in PSLBs was investigated by SFVS. DPPS was incorporated into bilayers composed of 1,2-distearoyl-*sn*-glycero-3-phosphocholine (DSPC). The use of DSPC offers several advantages to the present study, the first of which being that the matched gel to liquid-crystalline phase transition temperatures (T_m) of DSPC and DPPS promotes miscibility and stability of the lipid mixtures. Second, previous studies have thoroughly investigated the energetics of DSPC lipid flip-flop,[32,33] making it possible to isolate the impact of DPPS on membrane dynamics in the present work. In the discussion that follows, we report the kinetics and transition-state thermodynamics for the individual PS and PC components of these bilayers in order to quantify the impact of PS content on membrane lipid flip-flop dynamics.

THEORY

The full theory of SFVS has been presented elsewhere,[39−41] and only the pertinent aspects will be discussed here. SFVS is a nonlinear, optical technique that involves the spatial and temporal overlap of a fixed visible and tunable IR laser source to produce a third beam whose frequency is the sum of the two input frequencies. The intensity of the sum frequency, I_{SF}, is proportional to the second-order nonlinear susceptibility tensor, $\chi^{(2)}$, according to

$$I_{SF} \propto |\chi^{(2)}| \tag{1}$$

The susceptibility tensor is described by

$$|\chi^{(2)}| \propto \frac{N\langle A_k M_{ij}\rangle}{\omega_\nu - \omega_{IR} - i\Gamma_\nu} \tag{2}$$

where N is the number of molecules at the interface, A_k and M_{ij} are the IR and Raman transition probabilities, respectively, ω_ν and Γ_ν are the frequency and line width of the vibrational transitions of the molecule, respectively, and ω_{IR} is the frequency of the input IR beam. The bra-ket notation in eq 2 indicates that I_{SF} is dependent on the orientational average of the transition dipole moments in the sample. In an ensemble composed of equal populations of oppositely oriented dipoles, no net sum-frequency generation (SFG) is observed. The symmetry constraints on $\chi^{(2)}$ also make SFVS exquisitely sensitive to interfaces between two isotropic media where the inversion symmetry of the bulk phase is broken.

For lipids, the intensity of the terminal methyl symmetric stretch (CH_3 ν_s) originating from the acyl chains can be related to the lipid population difference between lipids in the top (N_T) and bottom (N_B) leaflets:

$$I_{CH_3} \propto |N_T - N_B|^2 \tag{3}$$

Typically, a bilayer contains equal amounts of lipids in both leaflets and the transition dipoles from oppositely oriented CH_3 ν_s from the acyl chains cancel.[33,42] The symmetry of the system can be broken by isotopically substituting deuterated acyl chains for proteated ones. The CD_3 ν_s is shifted to lower energy relative to the CH_3 ν_s, giving rise to a nonzero difference in the lipid distribution.

When the deuterated lipids in a bilayer are confined to one leaflet, a maximum population difference exists and the resulting SFVS signal is at a maximum, I_{max}. The population difference and corresponding SFVS signal decrease as lipids undergo flip-flop and proteated and deuterated lipids mix between the two leaflets. An integrated rate equation can be derived from eq 3 to relate the decay of I_{CH_3} as a function of time (t) to the rate of lipid flip-flop according to

$$I_{CH_3}(t) = I_{max}e^{-4kt} + I_o \tag{4}$$

where I_o is the intensity offset and k is the rate constant for lipid flip-flop.[33] The rate of lipid flip-flop (k) is experimentally determined by monitoring I_{CH_3} as a function of time and fitting the resulting decay to eq 4.

The dynamics of lipid flip-flop can be examined in more detail by determining the activation free energy barrier ($\Delta G^{\ddagger}$), which is calculated from k at a fixed temperature using the Eyring equation (eq 5)

$$k = \frac{k_B T}{h}\exp\left(-\frac{\Delta G^{\ddagger}}{RT}\right) \tag{5}$$

where k_B is Boltzmann's constant, h is Planck's constant, R is the ideal gas constant, and T is the temperature in kelvin. Examination of the temperature dependence of $\Delta G^{\ddagger}$ for lipid flip-flop allows the activation enthalpy ($\Delta H^{\ddagger}$) and entropy ($\Delta S^{\ddagger}$) to be determined from a linear plot of $\Delta G^{\ddagger}$ versus temperature according to

$$\Delta G^{\ddagger} = \Delta H^{\ddagger} - T\Delta S^{\ddagger} \tag{6}$$

Selective lipid deuteration can be used to isolate the behavior of individual bilayer components. This is demonstrated in Figure 1, which shows the SFVS spectrum of a PSLB where one leaflet was composed of the deuterated counterpart to DSPC, 1,2-distearoyl(d70)-*sn*-glycero-3-phosphocholine (DSPCd70), and the opposite leaflet was composed of a mixture of DSPC and DPPS where only one of these lipid components was proteated. In this way, the impact of the PS headgroup content on both the PS and PC lipid dynamics can be determined.

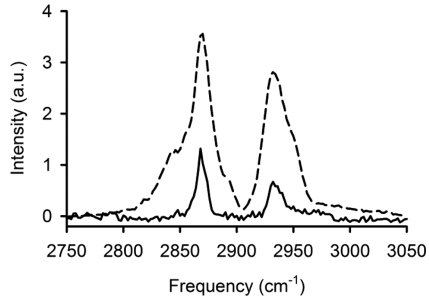

Figure 1. Representative SFVS spectra of the DPPS (solid) and DSPC (dashed) component of a bilayer with χ_{DPPS} = 0.05. The DPPS spectrum has been multiplied by a factor of 5 for clarity.

MATERIALS AND METHODS

Lipid Preparation. DSPC, 1,2-dipalmitoyl-*sn*-glycero-3-phosphocholine (DPPC), DPPS, and the deuterated counterparts DSPCd70 and 1,2-dipalmitoyl(d62)-*sn*-glycero-3-phospho-L-serine (DPPSd62) were obtained from Avanti Polar Lipids (Alabaster, AL) and used without further purification.

dx.doi.org/10.1021/jp409672q | J. Phys. Chem. B 2013, 117, 15041−15050

GC grade chloroform and methanol were obtained from Mallinckrodt (Phillipsburg, NJ) and used as received. Nanopure water (Barnstead Thermolyne, Dubuque, IA) was used with a minimum resistivity of 18.2 MΩ·cm. All lipid solutions were prepared at a concentration of 1 mg/mL. Binary lipid mixtures containing PS headgroup lipids were prepared from single lipid solutions in a 65:35:8 mixture of $CHCl_3$:MeOH:H_2O. The molar fractions of PS lipids used were 0.05, 0.1, 0.15, or 0.2. Binary lipid mixtures not containing PS headgroup lipids were prepared in $CHCl_3$. Solutions of single lipids were also prepared in $CHCl_3$.

Bilayer Preparation. PSLBs were prepared on hemicylindrical fused silica substrates (Almax Optics, Marlton, NJ). Substrates were cleaned overnight in a solution of 70% 18 M sulfuric acid and 30% H_2O_2. Immediately before use, substrates were rinsed with copious amounts of Nanopure water and cleaned in argon plasma for 2−4 min. PSLBs were prepared on a KSV Instruments minitrough (Helsinki, Finland) in a subphase of Nanopure water adjusted to pH = 7.0 ± 0.3 using dilute NaOH (Mallinckrodt, Phillipsburg, NJ).

Bilayers were prepared via the Langmuir−Blodgett/Langmuir−Schaeffer deposition method, which has been described in detail elsewhere.[32,33] Briefly, a monolayer of lipids was spread at the air−water interface of a Langmuir trough. The lipid film was then compressed by Teflon barriers as the surface pressure was monitored by a Whilhelmy plate. After equilibrating at the desired surface pressure of 30 mN/m, the substrate was slowly withdrawn through the interface to deposit the LB layer (proximal leaflet). The LS layer (distal leaflet) was deposited in a similar manner using a fresh subphase, new lipid solution, and horizontally submerging the prism through the interface. This method provides precise control over the packing and composition of the bilayer, allowing each leaflet to have a unique composition.

Unless otherwise noted, the LB layer of the PSLBs used here was composed of DSPCd70. The kinetics of DPPS flip-flop were measured using a DPPS + DSPCd70 mixture in the distal leaflet (Figure 2, top) while the kinetics of DSPC flip-flop were measured using a DPPCd62 + DSPC mixture (Figure 2, bottom). Following deposition, the bilayer was transferred to a custom-built Teflon flow cell and rinsed with D_2O (Cambridge Isotope Laboratories, Andover, MA) to avoid spectral interference.

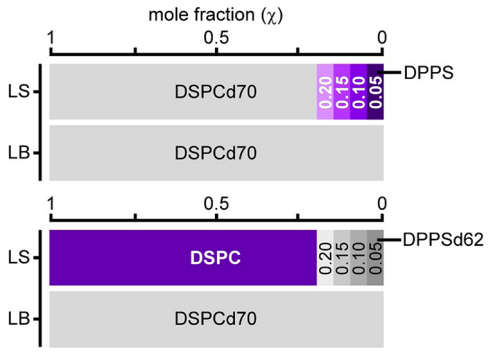

Figure 2. Graphical representation of the lipid distribution in the LB (proximal) and LS (distal) leaflets of the bilayer where χ_{DPPS} is varied from 0.05 to 0.20. The lipid fraction indicated in purple will give rise to the SFVS signal, which is used to selectively monitor the DPPS fraction (top) or the DSPC fraction (bottom).

Pressure−Area Isotherms. Pressure−area isotherms were performed on the LB trough to measure changes in packing density as a function of DPPS and DSPC lipid composition. A lipid monolayer was initially deposited at the air/water interface of the Langmuir trough at a low surface pressure (<1 mN/m) and compressed to collapse pressure (<50 mN/m). The surface pressure of the film was recorded as a function of the mean molecular area of the lipids to determine the packing density at 30 mN/m.

Sum-Frequency Vibrational Spectroscopy. SFVS measurements were performed using a custom-built OPO/OPA system (LaserVision, Bellevue, WA) pumped by the fundamental 1064 nm output of a 10 Hz Nd:YAG laser (Continuum, Santa Clara, CA) with a pulse duration of 7−9 ns and an energy of 500 mJ/pulse. The OPO/OPA produced tunable IR (5 mm^2, 3 mJ/pulse) and fixed 532 nm (10 mm^2, 8 mJ/pulse) beams which were directed at the SiO_2/D_2O interface through the prism with incident angles of 61° and 66°, respectively. The spectrometer setup is described more fully elsewhere.[22] SFVS spectra were collected by scanning the incident IR frequency in 2 cm^{-1} steps and integrating 30 laser pulses. In order to selectively probe vibrational transitions parallel to the surface normal, the ssp polarization combination was used (sum-frequency, 532 nm, IR) for all experiments.

Measurement of Lipid Flip-Flop Kinetics. Lipid bilayers were heated to a fixed temperature using a circulating water bath (HAAKE Phoenix II P1 Circulator, Thermo Fisher Scientific) while the SFVS intensity was monitored at the CH_3 ν_s frequency (2875 cm^{-1}). The temperature in the flow cell was monitored by a thermocouple, and all data points prior to temperature equilibration were discarded. The SFVS intensity decay curves were fit to eq 4 to determine the rate of flip-flop for a given bilayer composition measured at a constant temperature. These experiments were performed for each DPPS + DSPC bilayer composition at five or more temperatures. Previous work has shown that flip-flop of fluid-phase lipids occurs too rapidly to be measured experimentally.[32,37] Accordingly, the experiments presented here were conducted below the T_m of all lipid components, and the bilayers were in the gel phase.

RESULTS AND DISCUSSION

SFVS Spectra of Lipid Bilayers. A representative SFVS spectrum of an asymmetric bilayer composed of DPPSd62 + DSPC ($\chi_{DPPSd62}$ = 0.05) in the distal leaflet and DSPCd70 in the proximal leaflet is given in Figure 1. Only the DSPC component of this bilayer is proteated, and all of the SFVS signal can be attributed to DSPC. Figure 1 also shows a representative spectrum for the same bilayer composition (χ_{DPPS} = 0.05) where only the DPPS component is proteated. The signal from the DPPS component is an order of magnitude lower than the DSPC component and has been multiplied by a factor of 5 for clarity. The difference in intensity is due to the direct relationship between the square of the number of lipids and the measured SFVS intensity (eqs 1 and 2). When monitoring the DPPS component, only 5% of the distal leaflet contributes to the SFVS signal as opposed to 95% when monitoring the complementary DSPC component (Figure 1). Despite this difference in intensity, both spectra show a strong resonance around 2875 cm^{-1} from the CH_3 ν_s. The peak at 2940 cm^{-1} observed in both spectra is assigned as a combination of the CH_3 Fermi resonance at 2905 cm^{-1} and the CH_2 asymmetric stretch at 2960 cm^{-1}.

dx.doi.org/10.1021/jp409672q | J. Phys. Chem. B 2013, 117, 15041−15050

The main spectral difference between the DPPS and DSPC components lies in the CH_2 ν_s resonance at 2850 cm^{-1}. The DSPC spectrum in Figure 1 exhibits a shoulder at this frequency typical of bilayers containing a small amount of disorder in the lipid acyl chains.[43] Although the corresponding DPPS spectrum does not contain this feature, it is difficult to draw any conclusions about the relative order of the bilayer components due to the significant reduction in overall intensity. However, the DPPS spectra for all χ_{DPPS} investigated here are of this shape (data not shown) so any possible structural changes are conserved across all bilayer compositions.

Kinetics of Lipid Flip-Flop. As described above, the rate of lipid flip-flop was determined by monitoring the CH_3 ν_s stretch at 2875 cm^{-1} as a function of time and temperature. Representative decay curves for DPPS at 39 °C are shown in Figure 3A. These data have been fit to eq 4, and the

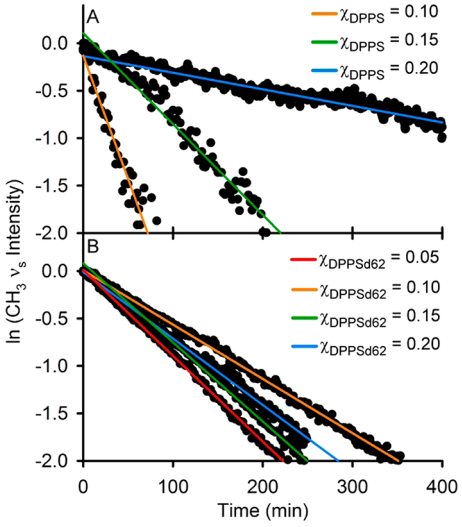

Figure 3. Representative CH_3 ν_s intensity decays for (A) the DPPS component of bilayers at 39 °C and (B) the DSPC component of bilayers at 42 °C. The solid lines are the fits to the data using eq 4.

corresponding rate constants for DPPS flip-flop are given in Table 1 as a function of temperature and bilayer composition. The half-life for decay is also included in Table 1, which was calculated using the following relationship:

$$t_{1/2} = \frac{\ln 2}{2k} \quad (7)$$

The data in Figure 3A indicate that the rate of DPPS flip-flop is strongly dependent on the amount of DPPS present in the bilayer. At the lowest mole fraction of DPPS (χ_{DPPS} = 0.05), DPPS flip-flop is extremely rapid with a half-life of only 37 min around 34 °C (Table 1). When χ_{DPPS} = 0.1, the rate of DPPS flip-flop decreases by an order of magnitude with a corresponding half-life of 229 min at 34 °C. This trend continues when the fraction of DPPS increases to 0.15 and 0.2 (Table 1), demonstrating that the rate of DPPS flip-flop is significantly influenced by small changes in the membrane composition.

The kinetic information given in Table 1 was collected well below the T_m of the lipids (54 °C) where the bilayers were in the gel phase. For all bilayer compositions investigated here, lipid flip-flop near the T_m occurs too quickly to be measured, suggesting that DPPS flip-flop in the fluid phase (above the T_m) is extremely rapid. While this is consistent with previous SFVS studies on gel phase lipids,[32,33] other reports of PS lipid flip-flop reported half-lives on the order of hours to days in the fluid phase.[44,45] However, these studies tracked the kinetics of fluorescent NBD−PS lipid analogues in PC lipid vesicles where the precise surface pressure was unknown.[44,45] Both the NBD label and packing density are known to impact the rate of lipid flip-flop[32,37,46] and likely contribute to these previously reported slow rates of PS lipid flip-flop. The work presented here monitors the rate of native lipid flip-flop in a well-controlled environment and shows for the first time that PS lipids undergo extremely rapid unassisted flip-flop in the gel phase of PSLBs.

The translocation of the complementary DSPC fraction of these mixed bilayers was investigated by deuterating the DPPS fraction, as denoted in Figure 2 (bottom). Figure 3B shows representative decay curves for DSPC flip-flop around 42 °C that have been fit to eq 4. The corresponding rates and half-lives are listed in Table 1. Unlike DPPS, the decays for DSPC flip-flop in Figure 3 are similar for all bilayer compositions (χ_{DPPS} = 0.05, 0.1, 0.15, and 0.2) and the half-lives are on the order of 200 min at 42 °C (Table 1). This indicates that the bulk DSPC lipid matrix is not appreciably impacted by the small amounts of DPPS incorporated into these bilayers. DSPC flip-flop also occurs much slower than DPPS flip-flop for most bilayer compositions. For example, when χ_{DPPS} = 0.10, the half-life of lipid flip-flop at 40 °C is 309 min for DSPC relative to 32 min for DPPS. This distinct behavior indicates that DPPS and DSPC undergo flip-flop separately in these mixed bilayers. Although this may seem indicative of domain formation, it is unlikely given the miscibility of DPPS and DSPC in these bilayers coupled with the inherent repulsion of the negatively charged PS headgroups. Rather, the distinct kinetics observed for DPPS and DSPC lipids here are suggestive of a unimolecular mechanism for lipid flip-flop.

Activation Energy for Lipid Flip-Flop. The activation free energy ($\Delta G^{\ddagger}$) for lipid flip-flop was calculated from the rate constants via eq 5 and plotted as a function of temperature in Figure 4. The data were fit to eq 6, and the fit for DSPC flip-flop in single-component bilayers determined from our previous work was included as a reference for the bulk DSPC matrix in the DPPS + DSPC bilayers.[32] The top panel of Figure 4 shows that the activation free energies for DSPC flip-flop when χ_{DPPS} = 0.05 (open triangles) lie on or near the fit for DSPC flip-flop in single-component bilayers. This similarity can be further assessed by extrapolating $\Delta G^{\ddagger}$ for DSPC flip-flop to the physiological temperature of 37 °C from the fit to eq 6. These values are given in Table 2 and show that the $\Delta G^{\ddagger}$ for DSPC flip-flop when χ_{DPPS} = 0.05 (106 ± 2 kJ/mol) is statistically identical to that of single-component DSPC bilayers (107 ± 2 kJ/mol).[32] Figure 4 also shows that there is no appreciable change in the activation free energies for DSPC flip-flop as the fraction of DPPS increases from 0.05 (top) to 0.2 (bottom), and the $\Delta G^{\ddagger}$ at 37 °C for DSPC flip-flop is 105−106 kJ/mol for all bilayer compositions. Therefore, the energetics of DSPC flip-flop are not only unaffected by the inclusion of PS lipids but, more strikingly, the activation free energy and kinetic rates are identical to those measured for a single-component DSPC bilayer.

Conversely, Figure 4 (top) shows that the activation free energy for DPPS flip-flop when χ_{DPPS} = 0.05 (solid circles) deviates from the bulk DSPC matrix and is shifted to a substantially lower energy with a calculated $\Delta G^{\ddagger}$ at 37 °C of

dx.doi.org/10.1021/jp409672q | J. Phys. Chem. B 2013, 117, 15041−15050

Table 1. Kinetics of DPPS and DSPC Flip-Flop[a]

LS leaflet composition	T (°C)	k (s^{-1}) × 10^5	$t_{1/2}$ (min)	LS leaflet composition	T (°C)	k (s^{-1}) × 10^5	$t_{1/2}$ (min)
χ_{DPPS} = **0.05**,	25.6	1.77 ± 0.07	326 ± 14	$\chi_{DPPSd62}$ = 0.05,	38.6	1.09 ± 0.01	532 ± 5
$\chi_{DSPCd70}$ = 0.95	27.5	3.3 ± 0.1	175 ± 5	χ_{DSPC} = **0.95**	41.2	2.64 ± 0.03	219 ± 2
	30.01	7.6 ± 0.3	76 ± 3		42.0	3.75 ± 0.01	154.0 ± 0.4
	32.23	13 ± 2	44 ± 7		45.1	5.22 ± 0.04	111 ± 1
	33.6	15.5 ± 1.0	37 ± 2		47.6	11.7 ± 0.1	49 ± 1
χ_{DPPS} = **0.10**,	33.98	2.520 ± 0.003	229 ± 2	$\chi_{DPPSd62}$ = 0.10,	38.56	1.30 ± 0.03	444 ± 9
$\chi_{DSPCd70}$ = 0.90	35.4	3.6 ± 0.1	160 ± 5	χ_{DSPC} = **0.90**	40.3	1.87 ± 0.02	309 ± 4
	38.5	12.2 ± 0.1	47 ± 2		42.0	2.39 ± 0.01	242 ± 1
	39.8	17.8 ± 0.1	32 ± 2		44.0	4.93 ± 0.04	117 ± 1
	41.1	23.7 ± 0.8	24 ± 1		45.7	5.37 ± 0.05	107 ± 1
					47.0	14.3 ± 0.2	40.4 ± 0.7
χ_{DPPS} = **0.15**,	35.05	0.6 ± 0.3	895 ± 346	$\chi_{DPPSd62}$ = 0.15,	37.82	1.07 ± 0.02	539 ± 12
$\chi_{DSPCd70}$ = 0.85	36.4	1.16 ± 0.03	500 ± 28	χ_{DSPC} = **0.85**	38.7	2.00 ± 0.01	288 ± 2
	39.26	3.3 ± 0.2	173 ± 11		41.05	3.34 ± 0.01	172.9 ± 0.5
	40.1	5.71 ± 0.02	101 ± 4		45.1	7.8 ± 0.3	74 ± 3
	41.7	10.4 ± 0.6	56 ± 3		46.9	9.9 ± 0.2	58.4 ± 0.9
	42.6	15.0 ± 0.5	39 ± 1				
χ_{DPPS} = **0.20**,	38.9	0.78 ± 0.03	740 ± 25	$\chi_{DPPSd62}$ = 0.20,	37.06	1.12 ± 0.005	516 ± 2
$\chi_{DSPCd70}$ = 0.80	42.4	2.30 ± 0.08	251 ± 8	χ_{DSPC} = **0.80**	40.2	3.99 ± 0.007	144.8 ± 0.2
	44.2	3.9 ± 0.3	147 ± 8		41.7	2.95 ± 0.05	196 ± 3
	44.9	6.2 ± 0.2	94 ± 4		42.5	5.49 ± 0.05	105.2 ± 0.9
	47.2	11.3 ± 0.4	51 ± 2		45.0	7.20 ± 0.07	80.2 ± 0.8
					47.2	19.1 ± 0.3	30.2 ± 0.4

[a]Kinetics of DPPS and DSPC flip-flop in mixed DPPS + DSPC bilayers as a function of the bilayer composition. The lipid component measured is indicated in bold.

95.5 ± 0.5 kJ/mol. As the fraction of DPPS increases, the activation free energy for DPPS flip-flop shifts to higher energy and eventually coincides with that measured for pure DSPC (Figure 4). Table 2 shows that the $\Delta G^{\ddagger}$ for DPPS flip-flop at 37 °C increase to 100.8 ± 0.4, 104.8 ± 0.3, and 108.1 ± 0.9 kJ/mol when χ_{DPPS} is 0.1, 0.15, and 0.2, respectively. This demonstrates that the energetics of DPPS flip-flop are drastically impacted by the fraction of DPPS in the membrane. This behavior is in stark contrast to the DSPC energetics, which remain unchanged for the same bilayer compositions. However, it is not clear whether this is the result of the PS headgroup. As previously noted, DPPS and DSPC were selected for this study because they are phase matched. Consequently, both the headgroups (PS versus PC) and acyl chain lengths (16 versus 18 carbons) are mismatched in these bilayers. The impact of chain length and headgroup on lipid flip-flop was explicitly investigated and is discussed below.

Headgroup versus Acyl Chain Length. The impact of the lipid headgroup on the energetics of DPPS flip-flop was directly investigated by replacing the bulk DSPC matrix with its 16-carbon acyl chain counterpart, DPPC. The fraction of DPPS was again varied from 0.05 to 0.2, and the $\Delta G^{\ddagger}$s for DPPS flip-flop are shown in Figure 4 (black squares). Figure 4 also includes the fit to the activation free energies for DPPC flip-flop in a single-component bilayer (solid gray) as a reference point.[32] The $\Delta G^{\ddagger}$ for DPPS flip-flop at 29 °C in these chain length matched bilayers is ~100 kJ/mol and does not change as a function of DPPS concentration (Figure 4). Furthermore, these values lie on or near the fit for pure DPPC bilayers and are within error of the $\Delta G^{\ddagger}$ for DPPC flip-flop at 29 °C (98.2 ± 0.5 kJ/mol).[32] This shows that DPPS behaves the same as the bulk DPPC matrix, and the PS headgroup does not appreciably influence the energetics of DPPS flip-flop at these low mole fractions.

The role of acyl chain length was investigated by replacing DPPS with its PC headgroup counterpart, DPPC. In these bilayers, the PC headgroup was conserved while the acyl chain lengths were mismatched. The fraction of DPPC was varied from 0.05 to 0.2 to mimic the DPPS fraction in previous bilayers. The $\Delta G^{\ddagger}$s for DPPC flip-flop in these mixed bilayers are plotted in Figure 4 (gray triangles) and show good agreement with DPPS flip-flop when $\chi_{DPPC} = \chi_{DPPS}$. This suggests that the changes in $\Delta G^{\ddagger}$ observed for DPPS flip-flop in DPPS + DSPC bilayers are driven by the two-carbon mismatch in the acyl chains. This finding is surprising given that nearly all previous studies on acyl chain mismatch investigate a minimum difference of four carbons to see any significant change in lipid properties.[47−49] The few studies that do investigate a two-carbon acyl chain mismatch examine biologically unrealistic mole fractions (0.25−0.75) and report that bulk lipid properties, such as lipid order and vesicle size, are dictated by the majority lipid.[49,50]

Although existing studies on chain length mismatch do not explain the DPPS energetics in DPPS + DSPC bilayers measured here, a previous SFVS study on mixed DSPC + DSPE bilayers may provide some insight. Anglin et al. showed that the energetics of DSPC and DSPE flip-flop in mixed bilayers were dictated by changes in the lipid packing as the fraction of DSPE was increased from 0.1 to 1.[37] The magnitude of the changes in $\Delta G^{\ddagger}$ observed for the DSPC + DSPE mixed bilayers is on the same order of magnitude as those reported here.[37] As a result, the role of lipid packing on the energetics of DSPC and DPPS flip-flop was investigated.

Pressure−Area Isotherms of DPPS + DSPC Mixtures. Pressure−area isotherms were performed on the DPPS + DSPC mixtures, and the average molecular area at 30 mN/m is given as a function of bilayer composition in Table 3. When χ_{DPPS} = 0.05, the mean molecular area of the DPPS + DSPC

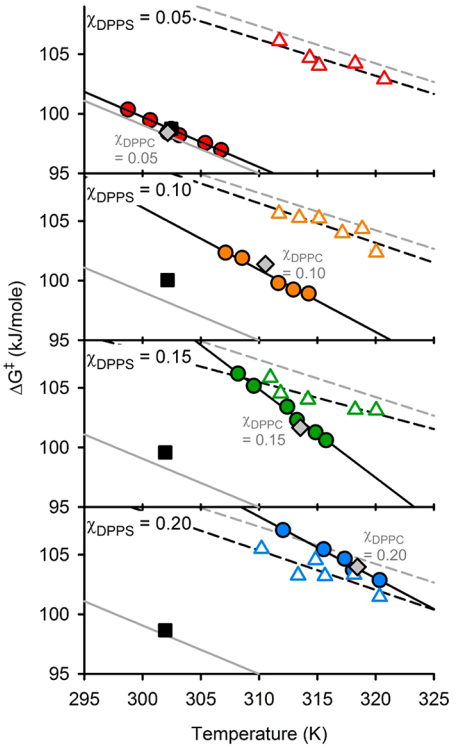

Figure 4. Activation free energy plots for DPPS + DSPC bilayers with χ_{DPPS} = 0.05 (red), 0.1 (orange), 0.15 (green), or 0.2 (blue). The solid circles refer to the DPPS component, and the open triangles refer to the DSPC component. The solid black and dashed black lines are the fits to eq 6 for the DPPS and DSPC data, respectively. The black squares represent chain length matched bilayers composed of DPPS + DPPC. The gray diamonds represent headgroup matched bilayers composed of DPPC + DSPC where χ_{DPPC} is equal to the χ_{DPPS} indicated on each graph. The fits to eq 6 for single-component DSPC (dashed gray) and DPPC (solid gray) have been included as previously determined in ref 32.

monolayer is 40.0 ± 1.6 Å^2/molecule. This is 9.1 Å^2/molecule smaller than a single-component DSPC film, and the corresponding $\Delta G^{\ddagger}$ for DPPS flip-flop decreases 11.5 kJ/mol. The mean molecular area of the DPPS + DSPC films expanded to 41.2 ± 1.2 and 42.5 ± 0.8 Å^2/molecule when χ_{DPPS} was 0.1 and 0.15, respectively, but compressed to 41.3 ± 2.5 Å^2/molecule when χ_{DPPS} was 0.2.

The impact of these changes in lipid packing were examined by plotting $\Delta G^{\ddagger}$ for lipid flip-flop as a function of molecular area (Figure 5). These data show that there is a linear correlation between lipid packing and the energetics of DPPS flip-flop when χ_{DPPS} is 0.05 (red), 0.1 (orange), and 0.15 (green) with $\Delta G^{\ddagger}$ increasing as the mean molecular area increases. The magnitude of this correlation was evaluated by fitting the data in Figure 5 to obtain a slope of 3.7 ± 0.6. Interestingly, the correlation between molecular area and $\Delta G^{\ddagger}$ for DSPC + DSPE bilayers had a slope of −1.65 ± 0.08,[37] representing a weaker dependence where the $\Delta G^{\ddagger}$ decreases as the molecular area increased. Furthermore, Figure 5 shows that the $\Delta G^{\ddagger}$ for DPPS flip-flop when χ_{DPPS} = 0.2 deviates from the linear trend. This is in contrast to the DSPC + DSPE study, where it was observed that the $\Delta G^{\ddagger}$ correlated linearly with the molecular area for all bilayer compositions.[37]

As discussed previously, the $\Delta G^{\ddagger}$ for DSPC flip-flop remains statistically identical to that of single-component DSPC bilayers and, consequently, shows no correlation with the changes in

Table 2. Transition-State Thermodynamics for DPPS and DSPC[a]

LS leaflet composition	$\Delta G^{\ddagger}$ (kJ/mol)[b]	$\Delta H^{\ddagger}$ (kJ/mol)	$\Delta S^{\ddagger}$ (J/(mol K))	$T\Delta S^{\ddagger}$ (kJ/mol)[b]
χ_{DPPS} = **0.05**, $\chi_{DSPCd70}$ = 0.95	95.5 ± 0.5	226 ± 6	421 ± 21	131 ± 7
$\chi_{DPPSd62}$ = 0.05, χ_{DSPC} = **0.95**	106 ± 2	201 ± 24	305 ± 76	94 ± 24
χ_{DPPS} = **0.10**, $\chi_{DSPCd70}$ = 0.90	100.8 ± 0.4	262 ± 13	522 ± 42	162 ± 13
$\chi_{DPPSd62}$ = 0.10, χ_{DSPC} = **0.90**	106 ± 2	210 ± 27	333 ± 87	103 ± 27
χ_{DPPS} = **0.15**, $\chi_{DSPCd70}$ = 0.85	104.8 ± 0.3	335 ± 9	742 ± 28	230 ± 9
$\chi_{DPPSd62}$ = 0.15, χ_{DSPC} = **0.85**	105 ± 1	187 ± 21	262 ± 66	81 ± 21
χ_{DPPS} = **0.20**, $\chi_{DSPCd70}$ = 0.80	108.1 ± 0.9	268 ± 13	517 ± 41	160 ± 13
$\chi_{DPPSd62}$ = 0.20, χ_{DSPC} = **0.80**	105 ± 2	208 ± 31	331 ± 97	103 ± 30
DSPC[c]	107 ± 2	204 ± 18	312 ± 57	97 ± 18

[a]Transition-state thermodynamics for DPPS and DSPC lipid flip-flop as a function of bilayer composition. The errors for $\Delta H^{\ddagger}$ and $\Delta S^{\ddagger}$ were determined from the linear regression of the data shown in Figure 4. The errors for $\Delta G^{\ddagger}$ represent the 95% confidence interval of the fit in Figure 4. [b]Values calculated at 37 °C. [c]Values extrapolated from the data given in ref 32.

Table 3. Mean Molecular Area per Lipid for DPPS + DSPC Lipid Films at 30 mN/m

lipid mixture	mean molecular area (Å^2/lipid)
χ_{DPPS} = 0.05, $\chi_{DSPCd70}$ = 0.95	40.0 ± 1.6
χ_{DPPS} = 0.10, $\chi_{DSPCd70}$ = 0.90	41.1 ± 1.2
χ_{DPPS} = 0.15, $\chi_{DSPCd70}$ = 0.85	42.5 ± 0.8
χ_{DPPS} = 0.20, $\chi_{DSPCd70}$ = 0.80	41.3 ± 2.5
DSPCd70	49.1 ± 1.9

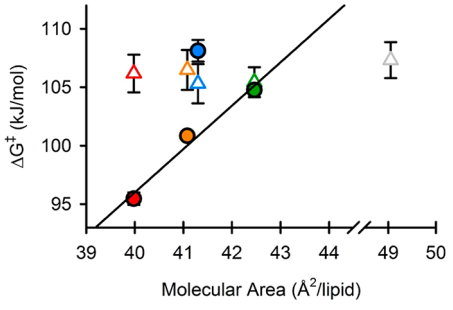

Figure 5. $\Delta G^{\ddagger}$ at 37 °C for DPPS flip-flop (solid circles) and DSPC flip-flop (open triangles) when χ_{DPPS} = 0.05 (red), 0.10 (orange), 0.15 (green), and 0.20 (blue) as a function of lipid mean molecular area at 30 mN/m. The data for single-component DSPC bilayers (gray open triangle) are included as determined in ref 32.

lipid packing. This is again unlike our previous study of DSPC + DSPE mixed bilayers, which reported equal changes in the energetics for both DSPC and DSPE flip-flop as a function of molecular area.[37] This indicates that the measured lipid packing for the DPPS + DSPC lipid mixtures does not represent an ensemble change but is limited to changes in only the local DPPS lipid environment. Taken together, this shows that the energetics of DPPS and DSPC flip-flop in binary membranes

dx.doi.org/10.1021/jp409672q | J. Phys. Chem. B 2013, 117, 15041−15050

cannot be fully explained by the lipid packing. In order to more fully describe the energetics of lipid flip-flop in these DPPS + DSPC bilayers, the activation entropy and enthalpy of lipid flip-flop were determined from eq 6 and are discussed in detail below.

Activation Enthalpy. The activation enthalpies of lipid flip-flop for the DPPS and DSPC components of these mixed bilayers were determined from the intercept of the fits in Figure 4, and the resulting values are given in Table 2. The activation enthalpy is mainly attributed to the energetic cost of moving the polar headgroup through the nonpolar membrane core and, in doing so, disrupting favorable H-bonding and van der Waals forces involved in solvent−lipid and lipid−lipid interactions. When χ_{DPPS} = 0.05, $\Delta H^{\ddagger}$ for DSPC flip-flop (201 ± 24 kJ/mol) is identical to that of a single-component DSPC bilayer (204 ± 18 kJ/mol).[32] Interestingly, the $\Delta H^{\ddagger}$ for DPPS flip-flop when χ_{DPPS} = 0.05 (226 ± 6 kJ/mol) is also similar to a single-component DSPC bilayer, suggesting that the DPPS lipid environment is not significantly different from the bulk DSPC matrix. This supports the previous assertion that DPPS is well dispersed in the DSPC matrix since changes in $\Delta H^{\ddagger}$ would be significantly altered by any domain formation or direct PS−PS interactions.

The $\Delta H^{\ddagger}$ for DPPS flip-flop increases to 262 ± 13 and 335 ± 9 kJ/mol when χ_{DPPS} is 0.1 and 0.15, respectively. While this substantial increase in $\Delta H^{\ddagger}$ may seem indicative of domain formation, Table 2 shows that this trend does not continue when χ_{DPPS} is 0.2 ($\Delta H^{\ddagger}$ = 268 ± 13 kJ/mol). This is unlike the trend observed for the $\Delta G^{\ddagger}$ of DPPS flip-flop, which increased continuously with χ_{DPPS}. In order to see if there is instead a correlation with the lipid packing, $\Delta H^{\ddagger}$ is plotted as a function of mean molecular area in Figure 6 (top). These data show that

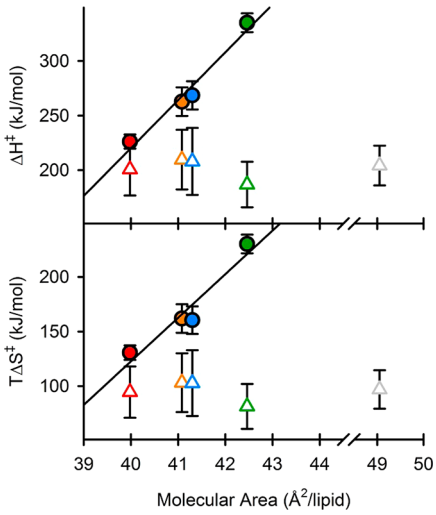

Figure 6. $\Delta H^{\ddagger}$ (top) and $T\Delta S^{\ddagger}$ at 37 °C (bottom) for DPPS (solid circles) and DPSC (open triangles) in DPPS + DSPC bilayers as a function of the mean molecular area at 30 mN/m. The data for single-component DSPC bilayers (open gray triangles) have been extrapolated from ref 32.

$\Delta H^{\ddagger}$ for DPPS flip-flop increases linearly with molecular area for all bilayer compositions examined here. Conversely, Table 2 shows that the $\Delta H^{\ddagger}$ for DSPC flip-flop does not change as a function of bilayer composition and is not correlated with the molecular area (Figure 6, top). This reiterates not only that the energetics of DSPC are not discernibly impacted by the incorporation of DPPS in these bilayers but also that the measured changes in molecular area correspond to local changes in the DPPS packing.

Changes in flip-flop energetics due to lipid packing have been previously attributed to the work term, $\pi\Delta a^{\ddagger}$, where π is the pressure of the bilayer and $\Delta a^{\ddagger}$ is the difference between the ground state and transition state geometries.[32,37] Figure 4 shows that single-component DPPC and DSPC bilayers are suitable metrics for the range of DPPS energetics observed here and can be used to estimate a potential contribution from $\pi\Delta a^{\ddagger}$, which is on the order of 10 kJ/mol.[32] This is an order of magnitude lower than the measured changes in $\Delta H^{\ddagger}$ for DPPS flip-flop, illustrating that the energetics for DPPS flip-flop must be driven by enthalpy, not the work term. Furthermore, the correlation between $\Delta H^{\ddagger}$ and molecular area has a slope of 44 ± 6, which is an order of magnitude larger than that observed for $\Delta G^{\ddagger}$ in Figure 5. In order to account for the relatively small changes in $\Delta G^{\ddagger}$ shown in Table 2, these large changes in $\Delta H^{\ddagger}$ must be counterbalanced by $\Delta S^{\ddagger}$. Consequently, the entropic contribution to DPPS flip-flop is discussed below.

Activation Entropy. The activation entropies of DPPS and DSPC flip-flop were determined from the slope of the fits in Figure 4 and are given in Table 2. The total contribution to the activation free energy at 37 °C, $T\Delta S^{\ddagger}$, is also included. The activation entropy for lipid flip-flop represents the difference in entropy between a lipid in the ground state and transition state geometry. The measured $T\Delta S^{\ddagger}$ for DSPC flip-flop in these mixed bilayers does not change relative to pure DSPC (97 ± 18 kJ/mol) or as a function of χ_{DPPS}. The correlation between $T\Delta S^{\ddagger}$ for lipid flip-flop and molecular area is plotted in Figure 6 (bottom) and shows that the unchanged DSPC energetics are unrelated to the lipid packing. This is in good agreement with the previous assertion that the measured changes in DPPS + DSPC packing are isolated to the DPPS component.

Relative to a single-component DSPC bilayer, $T\Delta S^{\ddagger}$ for DPPS flip-flop when χ_{DPPS} is 0.05 increases to 131 ± 7 kJ/mol as the molecular area decreases to 40 Å^2/molecule (Table 3). This is consistent with previous work showing that a smaller molecular area results in a higher $T\Delta S^{\ddagger}$ as more energy is required to accommodate the large transition-state geometry.[32] Figure 6 (bottom) shows that $T\Delta S^{\ddagger}$ for DPPS flip-flop increases linearly with molecular area when χ_{DPPS} is 0.1 (162 ± 13 kJ/mol), 0.15 (230 ± 9 kJ/mol), and 0.2 (160 ± 13 kJ/mol). Additionally, the correlation between $T\Delta S^{\ddagger}$ and the molecular area has a slope of 40 ± 8 to balance the changes in $\Delta H^{\ddagger}$ and account for the moderate changes in the $\Delta G^{\ddagger}$ for DPPS flip-flop. This suggests that the small changes in lipid packing may be symptomatic of a significant change in the bilayer that would impact both the entropy and enthalpy. This possibility was further investigated by quantifying the enthalpy−entropy compensation for DPPS flip-flop.

Enthalpy−Entropy Compensation. Figure 7 shows that a linear relationship exists between $\Delta H^{\ddagger}$ and $T\Delta S^{\ddagger}$ for DPPS flip-flop in a DSPC matrix. Previous studies have shown that systems subject to transition-state theory sometimes exhibit enthalpy−entropy compensation according to

$$T\Delta S^{\ddagger} = \alpha\Delta H^{\ddagger} + T\Delta S_0^{\ddagger} \quad (8)$$

The degree to which the entropy compensates the enthalpy is given by α where a value of 1 is representative of complete compensation.[51−54] The extent of enthalpy−entropy compensation in DPPS flip-flop here was assessed by fitting the data in Figure 7 to eq 8. The calculated α of 1.07 ± 0.08 shows that the

dx.doi.org/10.1021/jp409672q | J. Phys. Chem. B 2013, 117, 15041−15050

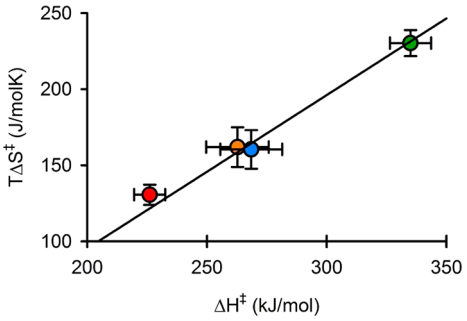

Figure 7. Enthalpy−entropy compensation plot for the DPPS component of DPPS + DSPC bilayers where χ_{DPPS} = 0.05 (red), 0.10 (orange), 0.15 (green), and 0.20 (blue). The solid line is the fit to eq 8.

$\Delta H^{\ddagger}$ for DPPS flip-flop is almost exactly compensated by $\Delta S^{\ddagger}$. For aqueous, biochemical systems, this compensation is often attributed to the "solvation effect" in which the enthalpy and entropy of solvent reorganization simultaneously affect both $\Delta H^{\ddagger}$ and $\Delta S^{\ddagger}$.[53,55,56]

Although the solvation effect is traditionally associated with protein folding, it is known to generate large changes in $\Delta H^{\ddagger}$ and $\Delta S^{\ddagger}$ that cancel to cause small changes in the overall $\Delta G^{\ddagger}$.[53] As discussed earlier, this is observed here as $\Delta H^{\ddagger}$ and $T\Delta S^{\ddagger}$ for DPPS flip-flop increase by about 100 kJ/mol while $\Delta G^{\ddagger}$ only increases by about 12 kJ/mol. Additionally, solvation driven enthalpy−entropy compensation often shows no correlation between $\Delta H^{\ddagger}$ and $\Delta G^{\ddagger}$ or $\Delta S^{\ddagger}$ and $\Delta G^{\ddagger}$.[53,57] Figures 5 and 6 show that this also occurs for DPPS flip-flop as $\Delta H^{\ddagger}$ and $T\Delta S^{\ddagger}$ increase linearly with molecular area and $\Delta G^{\ddagger}$ does not.

To the authors' knowledge, enthalpy−entropy compensation has never been reported for lipid flip-flop. It is important to note that it is not inherently clear what bilayer property would result in such a strong solvation effect due to the incorporation of small quantities of DPPS. It is possible that the DPPS lipids in these mixed bilayers experience stronger or more numerous interactions with the surrounding water molecules. This could increase $\Delta H^{\ddagger}$ (larger energetic penalty to break favorable interactions) as well as $\Delta S^{\ddagger}$ (higher degree of water reorganization in the transition state). Furthermore, this could also result in slight perturbations of the lipid packing as the molecular area increases to accommodate more water molecules. Although, this hypothesis cannot be directly evidenced by the data here, it is the most inclusive explanation of all the data.

CONCLUSIONS

SFVS was used here to quantify the kinetics and transition-state thermodynamics of lipid flip-flop in DPPS + DSPC bilayers where χ_{DPPS} was varied from 0.05 to 0.2. This work has shown that DPPS lipids in these mixed bilayers experience distinct energetics dependent on the fraction of DPPS incorporated in the bilayer. At the lowest fraction of DPPS, χ_{DPPS} = 0.05, DPPS flip-flop occurred an order of magnitude faster than DSPC flip-flop and the corresponding $\Delta G^{\ddagger}$ at 37 °C was 10 kJ/mol lower than that of DSPC. As χ_{DPPS} was increased, the rate and $\Delta G^{\ddagger}$ for DPPS flip-flop increased continuously. Conversely, the energetics for DSPC flip-flop showed no significant changes with χ_{DPPS} and remained statistically identical to single-component DSPC bilayers. Control experiments revealed that these unique DPPS energetics were the result of the mismatched acyl chain lengths of DPPS and DSPC rather than the PS headgroup.

The energetics of DPPS flip-flop in these mixed bilayers was shown to be directly related to lipid packing. Small changes in the molecular area at different fractions of DPPS were accompanied by changes in the $\Delta H^{\ddagger}$ and $T\Delta S^{\ddagger}$ on the order of 100 kJ/mol. Changes of this magnitude have not been previously reported for such small changes in molecular area (1−2 Å^2/molecule); however, most studies on mixed lipid systems have been limited to relatively large fractions of the minority lipid (>0.25). Therefore, the work presented here shows for the first time that biologically relevant quantities of DPPS lipids are highly perturbative to the energetics of lipid flip-flop.

The correlation between the $\Delta H^{\ddagger}$ and $T\Delta S^{\ddagger}$ for DPPS flip-flop and molecular area are opposite those observed previously. This suggests that the changes in lipid packing are a side effect of the changes in the bilayer, causing these complex energetics for DPPS flip-flop. Although it is not possible to directly determine the mechanism by which the small fractions of DPPS impact the energetics of DPPS flip-flop in these DPPS + DSPC bilayers, the enthalpy−entropy compensation suggests that lipid hydration may be a key element. Again, most previous studies on mixed chain bilayers have been limited to relatively large fractions (>0.25) of the minority lipid and offer no additional insight into how the small fractions of DPPS may be perturbing the membrane. However, this comprehensive study quantifies the impact of biologically relevant fractions of PS lipids on the energetics of lipid flip-flop for the first time.

AUTHOR INFORMATION

Corresponding Author

*E-mail conboy@chem.utah.edu; Phone (801) 585-7957 (J.C.C.).

Notes

The authors declare no competing financial interest.

ACKNOWLEDGMENTS

This work was supported by funds from the National Science Foundation (1110351).

REFERENCES

(1) Balasubramanian, K.; Schroit, A. J. Aminophospholipid Asymmetry: A Matter of Life and Death. *Annu. Rev. Physiol.* **2003**, *65*, 701−734.

(2) Op den Kamp, J. A. F. Lipid Asymmetry in Membranes. *Annu. Rev. Biochem.* **1979**, *48*, 47−71.

(3) Yamaji-Hasegawa, A.; Ysujimoto, M. Asymmetric Distribution of Phospholipids in Biomembranes. *Biol. Pharm. Bull.* **2006**, *29*, 1547−1553.

(4) Devaux, P. F. Protein Involvement in Transmembrane Lipid Asymmetry. *Annu. Rev. Biophys. Biomol. Struct.* **1992**, *21*, 417−439.

(5) Kay, J. G.; Grinstein, S. Sensing Phosphatidylserine in Cellular Membranes. *Sensors* **2011**, *11*, 1744−1755.

(6) Nishizuka, Y. Intracellular Signaling by Hydrolysis of Phospholipids and Activation of Protein Kinase C. *Science* **1992**, *258*, 607−614.

(7) Bevers, E. M.; Comfurius, P.; Van Rijn, J. L. M. L.; Hemker, H. C.; Zwaal, R. F. A. Generation of Prothrombin-Converting Activity and the Exposure of Phosphatidylserine at the Outer Surface of Platelets. *Eur. J. Biochem.* **1982**, *122*, 429−436.

(8) Casciola-Rosen, L.; Rosen, A.; Petri, M.; Schlissel, M. Surface Blebs on Apoptotic Cells are Sites of Enhanced Procoagulant Activity: Implications for Coagulation Events and Antigenic Spread in

Systematic Lupus Erythematosus. *Proc. Natl. Acad. Sci. U. S. A.* **1996**, *93*, 1624−1629.
(9) Devaux, P. F. Static and Dynamic Lipid Asymmetry in Cell Membranes. *Biochemistry* **1991**, *30*, 1163−1173.
(10) Devaux, P. F.; Herrmann, A.; Ohlwein, N.; Kozlov, M. M. How Lipid Flippases Can Modulate Membrane Structure. *Biochim. Biophys. Acta, Biomembr.* **2008**, *1778*, 1591−1600.
(11) van Meer, G.; Voelker, D. R.; Feigenson, G. W. Membrane Lipids: Where They Are and How They Behave. *Nat. Rev. Mol. Cell Biol.* **2008**, *9*, 112−124.
(12) Tanaka, Y.; Schroit, A. J. Insertion of Fluorescent Phosphatidylserine into the Plasma Membrane of Red Blood Cells. Recognition by Autologous Macrophages. *J. Biol. Chem.* **1983**, *258*, 11335−11343.
(13) Fadok, V. A.; Voelker, D. R.; Campbell, P. A.; Cohen, J. J.; Bratton, D. L.; Henson, P. M. Exposure of Phosphatidylserine on the Surface of Apoptotic Lymphocytes Triggers Specific Recognition and Removal by Macrophages. *J. Immunol.* **1992**, *148*, 2207−2216.
(14) Henson, P. M.; Bratton, D. L.; Fadok, V. A. Apoptotic Cell Removal. *Curr. Biol.* **2001**, *11*, R795−R805.
(15) Savill, J. Apoptosis in Resolution of Inflammation. *J. Leukocyte Biol.* **1997**, *61*, 375−380.
(16) Sakurai, K.; Katoh, M.; Someno, K.; Fujimoto, Y. Apoptosis and Mitochondrial Damage in INS-1 Cells Treated with Alloxan. *Biol. Pharm. Bull.* **2001**, *24*, 876−882.
(17) Wilson, M. J.; Richter-Lowney, K.; Daleke, D. L. Hyperglycemia Induces a Loss of Phospholipid Asymmetry in Human Erythrocytes. *Biochemistry* **1993**, *32*, 11302−11310.
(18) Kuypers, F. A.; Lewis, R. A.; Hua, M.; Schott, M. A.; Discher, D.; Ernst, J. D.; Lubin, B. H. Detection of Altered Membrane Phospholipid Asymmetry in Subpopulations of Human Red Blood Cells Using Fluorescently Labeled Annexin V. *Blood* **1996**, *87*, 1179−1187.
(19) Wang, R. H.; Phillips, G., Jr.; Medof, M. E.; Mold, C. Activation of the Alternative Complement Pathway by Exposure of Phosphatidylethanolamine and Phosphatidylserine on Erythrocytes from Sickle Cell Disease Patients. *J. Clin. Invest.* **1993**, *92*, 1326−1335.
(20) Toti, F.; Satta, N.; Fressinaud, E.; Meyer, D.; Freyssinet, J.-M. Scott Syndrome, Characterized by Impaired Transmembrane Migration of Procoagulant Phosphatidylserine and Hemorrhagic Complications, Is an Inherited Disorder. *Blood* **1996**, *87*, 1409−1415.
(21) Zwaal, R. F. A.; Comfurius, P.; Bevers, E. M. Scott Syndrome, A Bleeding Disorder Caused by Defective Scrambling of Membrane Phospholipids. *Biochim. Biophys. Acta, Mol. Cell Biol. Lipids* **2004**, *1636*, 119−128.
(22) Brown, K. L.; Conboy, J. C. Electrostatic Induction of Lipid Asymmetry. *J. Am. Chem. Soc.* **2011**, *133*, 8794−8797.
(23) Daleke, D. L. Phospholipid Flippases. *J. Biol. Chem.* **2007**, *282*, 821−825.
(24) Papadopulos, A.; Vehring, S.; Lopez-Montero, I.; Kutschenko, L.; Stoeckl, M.; Devaux, P. F.; Kozlov, M.; Pomorski, T.; Herrmann, A. Flippase Activity Detected with Unlabeled Lipids by Shape Changes of Giant Unilamellar Vesicles. *J. Biol. Chem.* **2007**, *282*, 15559−15568.
(25) Pomorski, T.; Holthuis, J. C. M.; Herrmann, A.; van Meer, G. Tracking Down Lipid Flippases and Their Biological Functions. *J. Cell Sci.* **2004**, *117*, 805−813.
(26) Kay, J. G.; Koivusalo, M.; Ma, X.; Wohland, T.; Grinstein, S. Phosphatidylserine Dynamics in Cellular Membranes. *Mol. Biol. Cell* **2012**, *23*, 2198−2212.
(27) Coleman, J. A.; Kwok, M. C. M.; Molday, R. S. Localization, Purification, and Functional Reconstitution of the P4-ATPase Atp8a2, a Phosphatidylserine Flippase in Photoreceptor Disc Membranes. *J. Biol. Chem.* **2009**, *284*, 32670−32679.
(28) Colleau, M.; Herve, P.; Fellmann, P.; Devaux, P. F. Transmembrane Diffusion of Fluorescent Phospholipids in Human Erythrocytes. *Chem. Phys. Lipids* **1991**, *57*, 29−37.
(29) Kornberg, R. D.; McConnell, H. M. Inside-Outside Transitions of Phospholipids in Vesicle Membranes. *Biochemistry* **1971**, *10*, 1111−1120.
(30) Romsicki, Y.; Sharom, F. J. Phospholipid Flippase Activity of the Reconstituted P-Glycoprotein Multidrug Transporter. *Biochemistry* **2001**, *40*, 6937−6947.
(31) Anglin, T. C.; Conboy, J. C. Lateral Pressure Dependence of the Phospholipid Transmembrane Diffusion Rate in Planar-Supported Lipid Bilayers. *Biophys. J.* **2008**, *95*, 186−193.
(32) Anglin, T. C.; Cooper, M. P.; Li, H.; Chandler, K.; Conboy, J. C. Free Energy and Entropy of Activation for Phospholipid Flip-Flop in Planar Supported Lipid Bilayers. *J. Phys. Chem. B* **2010**, *114*, 1903−1914.
(33) Liu, J.; Conboy, J. C. 1,2-Diacyl-phosphatidylcholine Flip-Flop Measured Directly by Sum-Frequency Vibrational Spectroscopy. *Biophys. J.* **2005**, *89*, 2522−2532.
(34) Lopez-Montero, I.; Rodriguez, N.; Cribier, S.; Pohl, A.; Velez, M.; Devaux, P. F. Rapid Transbilayer Movement of Ceramides in Phospholipid Vesicles and in Human Erythrocytes. *J. Biol. Chem.* **2005**, *280*, 25811−25819.
(35) Nakano, M.; Fukuda, M.; Kudo, T.; Endo, H.; Handa, T. Determination of Interbilayer and Transbilayer Lipid Transfers by Time-Resolved Small-Angle Neutron Scattering. *Phys. Rev. Lett.* **2007**, *98*, 238101/1−4.
(36) Lin, W.-C.; Blanchette, C. D.; Ratto, T. V.; Longo, M. L. Lipid Asymmetry in DLPC/DSPC-Supported Lipid Bilayers: A Combined AFM and Fluorescence Microscopy Study. *Biophys. J.* **2006**, *90*, 228−237.
(37) Anglin, T. C.; Conboy, J. C. Kinetics and Thermodynamics of Flip-Flop in Binary Phospholipid Membranes Measured by Sum-Frequency Vibrational Spectroscopy. *Biochemistry* **2009**, *48*, 10220−10234.
(38) Liu, J.; Conboy, J. C. Phase Behavior of Planar Supported Lipid Membranes Composed of Cholesterol and 1,2-Distearoyl-sn-glycerol-3-phosphocholine Examined by Sum-Frequency Vibrational Spectroscopy. *Vib. Spectrosc.* **2009**, *50*, 106−115.
(39) Chen, X.; Clarke, M. L.; Wang, J.; Chen, Z. Sum Frequency Generation Vibrational Spectroscopy Studies on Molecular Conformation and Orientation of Biological Molecules at Interfaces. *Int. J. Mod. Phys. B* **2005**, *19*, 691−713.
(40) Eisenthal, K. B. Interfaces Probed by Second-Harmonic and Sum-Frequency Spectroscopy. *Chem. Rev.* **1996**, *96*, 1343−1360.
(41) Lambert, A. G.; Davies, P. B. Implementing the Theory of Sum Frequency Generation Vibrational Spectroscopy: A Tutorial Review. *Appl. Spectrosc. Rev.* **2005**, *40*, 103−145.
(42) Liu, J.; Conboy, J. C. Direct Measurement of the Transbilayer Movement of Phospholipids by Sum-Frequency Vibrational Spectroscopy. *J. Am. Chem. Soc.* **2004**, *126*, 8376−8377.
(43) Liu, J.; Conboy, J. C. Structure of a Gel Phase Lipid Bilayer Prepared by the Langmuir-Blodgett/Langmuir-Schaefer Method Characterized by Sum-Frequency Vibrational Spectroscopy. *Langmuir* **2005**, *21*, 9091−9097.
(44) Sasaki, Y.; Shukla, R.; Smith, B. D. Facilitated Phosphatidylserine Flip-Flop Across Vesicle and Cell Membranes Using Urea-Derived Synthetic Translocases. *Org. Biomol. Chem.* **2004**, *2*, 214−219.
(45) Wimley, W. C.; Thompson, T. E. Transbilayer and Interbilayer Phospholipid Exchange in Dimyristoylphosphatidylcholine/Dimyristoylphosphatidylethanolamine Large Unilamellar Vesicles. *Biochemistry* **1991**, *30*, 1702−1709.
(46) Devaux, P. F.; Fellmann, P.; Herve, P. Investigation on Lipid Asymmetry Using Lipid Probes. Comparison Between Spin-labeled Lipids and Fluorescent Lipids. *Chem. Phys. Lipids* **2002**, *116*, 115−134.
(47) Bagatolli, L. A.; Gratton, E. A Correlation between Lipid Domain Shape and Binary Phospholipid Mixture Composition in Free Standing Bilayers: A Two-Photon Fluorescence Microscopy Study. *Biophys. J.* **2000**, *79*, 434−447.
(48) Lu, D.; Vavasour, I.; Morrow, M. R. Smoothed Acyl Chain Orientational Order Parameter Profiles in Dimyristoylphosphatidylcholine-Distearoylphosphatidylcholine Mixtures: A 2H-NMR Study. *Biophys. J.* **1995**, *68*, 574−583.

(49) Zheng, N.; Geehan, J.; Whitmore, M. D. Self-consistent Field Theory of Two-component Phospholipid Membranes. *Phys. Rev. E* **2007**, *75*, 051922/051921−051917.
(50) Ishii, F.; Nii, T. Properties of Various Phospholipid Mixtures as Emulsifiers or Dispersing Agents in Nanoparticle Drug Carrier Preparations. *Colloids Surf., B* **2005**, *41*, 257−262.
(51) Anbazhagan, V.; Sankhala, R. S.; Singh, B. P.; Swamy, M. J. Isothermal Titration Calorimetric Studies on the Interaction of the Major Bovine Seminal Plasma Protein, PDC-109 with Phospholipid Membranes. *PLoS One* **2011**, *6*, e25993/25991−25910.
(52) Inoue, Y.; Hakushi, T. Enthalpy-Entropy Compensation in Complexation of Cations with Crown Ethers and Related Ligands. *J. Chem. Soc., Perkin Trans. 2* **1985**, *0*, 935−946.
(53) Liu, L.; Guo, Q.-X. Isokinetic Relationship, Isoequilibrium Relationship, and Enthalpy-Entropy Compensation. *Chem. Rev.* **2001**, *101*, 673−695.
(54) Scott, M. J.; Jones, M. N. A Microcalorimetric Study of the Interaction of Phospholipid Liposomes with Colloidal Titanium Dioxide and Silica: An Example of Enthalpy−Entropy Compensation. *Colloids Surf., A* **2002**, *207*, 69−79.
(55) Fisicaro, E.; Compari, C.; Braibanti, A. Entropy/Enthalpy Compensation: Hydrophobic Effect, Micelles and Protein Complexes. *Phys. Chem. Chem. Phys.* **2004**, *6*, 4156−4166.
(56) Trzesniak, D.; van der Vegt, N. F. A.; van Gunsteren, W. F. Computer Simulation Studies on the Solvation of Aliphatic Hydrocarbons in 6.9 M Aqueous Urea Solution. *Phys. Chem. Chem. Phys.* **2004**, *6*, 697−702.
(57) Clay, A. T.; Sharom, F. J. Lipid Bilayer Properties Control Membrane Partitioning, Binding, and Transport of P-Glycoprotein Substrates. *Biochemistry* **2013**, *52*, 343−354.